AD-A262 177

UMENTATION PAGE

Form Approved
OBM No. 0704-0188

Report Date.	3. Report Type and Dates Covered.
April 1992	Final - Proceedings

4. Title and Subtitle.
Classification of Elastic Objects by Active Sonar in the Vicinity of Shallow Sea Boundaries

5. Funding Numbers

Contract	
Program Element No.	0601153N
Project No.	0302
Task No.	340
Accession No.	DN255011
Work Unit No.	12212B

6. Author(s).
Guillermo C. Gaunaurd* and Michael F. Werby

7. Performing Organization Name(s) and Address(es).
Naval Research Laboratory
Ocean Acoustics Branch
Stennis Space Center, MS 39529-5004

8. Performing Organization Report Number.
NRL/PP/7181--92-0001

9. Sponsoring/Monitoring Agency Name(s) and Address(es).
Naval Research Laboratory
Ocean Acoustics Branch
Stennis Space Center, MS 39529-5004

10. Sponsoring/Monitoring Agency Report Number.
NRL/PP/7181--92-0001

11. Supplementary Notes.
Published in SPIE.
*Naval Surface Warfare Center, Dahlgren Division, Code R42, White Oak Detachment, Silver Spring, MD 20902-5000 (USA)

12a. Distribution/Availability Statement.
Approved for public release; distribution is unlimited.

12b. Distribution Code.

13. Abstract *(Maximum 200 words).*

Active sonar classification of submerged elastic structures becomes increasingly difficult when the structure is close to the bottom or surface of the sea. The backscattering cross-section (BSCS) of any target, which is relatively simpler to determine in deep waters, away from boundaries, becomes substantially distorted as the structure approached either one of these environmental boundaries. Near these interfaces the classification methodology based on echo resonances that we have used in the past (viz., Appl. Mechanics Review 43, 171-208, (1990) can no longer be used. By means of the examples of a spherical shell and an elastic solid sphere insonified by plane waves, we study the above mentioned degradation in BSCS in order to assess how distant the structure should be from these boundaries before the resonance features become discernible again in the echoes, and object recognition is again possible. Our approach is based on the method of images for the construction of the appropriate Green's functions, combined with a very involved two-body scattering formulation that determines the combined T-Matrix of two insonified objects, when the T-Matrix of each individual object is known. The method is extended to the time domain. We present form-functions in the frequency domain, as well as late-time responses in the time domain for both sphere and shell as they approach the mentioned boundaries.

14. Subject Terms.
Acoustic scattering, shallow water, waveguide propagation

of Pages.
13

16. Price Code.

17. Security Classification of Report.	18. Security Classification of This Page.	19. Security Classification of Abstract.	20. Limitation of Abstract.
Unclassified	Unclassified	Unclassified	SAR

PROCEEDINGS
SPIE—The International Society for Optical Engineering

Automatic Object Recognition II

Firooz A. Sadjadi
Chair/Editor

22–24 April 1992
Orlando, Florida

Volume 1700

CLASSIFICATION OF ELASTIC OBJECTS BY ACTIVE SONAR IN THE VICINITY OF SHALLOW SEA BOUNDARIES

Guillermo C. Gaunaurd
Naval Surface Warfare Center
Dahlgren Division Code R42
White Oak Detachment
Silver Spring, MD 20903-5000
(USA)

Michael F. Werby
Naval Research Laboratory
Numerical Modeling
Division (221)
Stennis Space Center, MS 39529
(USA)

ABSTRACT

Active sonar classification of submerged elastic structures becomes increasingly difficult when the structure is close to the bottom or surface of the sea. The backscattering cross-section (BSCS) of any target, which is relatively simpler to determine in deep waters, away from boundaries, becomes substantially distorted as the structure approaches either one of these environmental boundaries. Near these interfaces the classification methodology based on echo resonances that we have used in the past (viz., Appl. Mechanics Reviews 43, 171-208, (1990)) can no longer be used. By means of the examples of a spherical shell and an elastic solid sphere insonified by plane waves, we study the above mentioned degradation in BSCS in order to assess how distant the structure should be from these boundaries before the resonance features become discernible again in the echoes, and object recognition is again possible. Our approach is based on the method of images for the construction of the appropriate Green's functions, combined with a very involved two-body scattering formulation that determines the combined T-Matrix of two insonified objects, when the T-Matrix of each individual object is known. The method is extended to the time domain. We present form-functions in the frequency domain, as well as late-time responses in the time domain for both sphere and shell as they approach the mentioned boundaries. Boundary effects seem to be confined to a "skin layer" bounded by $R \leq 4$. Within this layer the resonance features fade and are washed out in both the frequency and time domains. The formulation uses translation operators borrowed from atomic physics.

I. THEORETICAL APPROACH

The scattering of a plane c.w. scalar wavefield $\psi(\vec{r})$ by an object of surface S in an unbounded acoustic medium can be described by means of the T-Matrix method.[1] A brief review follows. The total wavefield is always the sum of the incident $\psi^i(\vec{r})$ and the scattered $\psi^s(\vec{r})$. Huygens principle states that[2]:

$$\psi^i(\vec{r}) + \iint_S [\psi(\vec{r}')\vec{\nabla}g(k|\vec{r}-\vec{r}'|) - \vec{\nabla}\psi(\vec{r}')g(k|\vec{r}-\vec{r}'|)] \cdot d\vec{S} = \begin{cases} \psi(\vec{r}) \\ 0 \end{cases} \qquad (1)$$

0-8194-0865-4/92/$4.00

whenever $\vec{r}$ is outside S (top formula) or $\vec{r}'$ is inside S (bottom). The three-dimensional Green's function for an unbounded space is[3]:

$$g(k|\vec{r}-\vec{r}'|) = \exp[ik|\vec{r}-\vec{r}'|]/4\pi|\vec{r}-\vec{r}'|, \tag{2}$$

which can be expanded in a complete set of solutions of Helmholtz equation $(\nabla^2+k^2)\psi(\vec{r})=0$, , which are, in normalized form:

$$\psi_{mn}(\vec{r}) \equiv \psi_{\{e\}mn}(\vec{r}) = \sqrt{\frac{\epsilon_m}{4\pi}(2n+1)}\sqrt{\frac{(n-m)!}{(n+m)!}}\,\rho_{mn}^{(1)}(kr)\,P_n^m(\cos\theta)\begin{Bmatrix}\cos m\phi\\ \sin m\phi\end{Bmatrix} \tag{3}$$

where $\epsilon_m=\begin{cases}1 & m=0\\ 2 & m\neq 0\end{cases}$; $\vec{r}(r,\theta,\phi)$, and e, o correspond to even or odd indices.[4] The desired expansion is:

$$g(k|\vec{r}-\vec{r}'|) = ik\sum_n \psi_n(k\vec{r}_>)\,\mathrm{Re}\,\psi_n(k\vec{r}_<) = \tag{4}$$

$$= ik\sum_{n=0}^{\infty}\sum_{m=0}^{n} A_{mn}\,h_m^{(1)}(kr_>)\,j_n(kr_<)\,P_n^m(\cos\theta_>)\,P_n^m(\cos\theta_<)\begin{Bmatrix}\cos m\phi_>\\ \sin m\phi_>\end{Bmatrix}\begin{Bmatrix}\cos m\phi_<\\ \sin m\phi_<\end{Bmatrix}$$

$$A_{mn} = \frac{\epsilon_m}{4\pi}(2n+1)\frac{(n-m)!}{(n+m)!} \tag{5}$$

We note that $\mathrm{Re}\psi_n(\vec{r})$ are like the $\psi_n(\vec{r})$, but with the $h_n^{(1)}(kr)$ replaced by their regular parts, $j_n(kr)$. [m=0,1,2,...n] The T-Matrix approach[1] gives the coefficients of the scattered field in terms of those of the incident, when both are expanded in terms of the above solutions in Equation (3). The scattered field admits the expansion:

$$\psi_s(\vec{r}) = \sum_n f_n\psi_n(\vec{r}), \tag{6}$$

and the incident field, analogously, the expansion:

$$\psi^i(\vec{r}) = \sum_n a_n\,\mathrm{Re}\psi_n(\vec{r}). \tag{7}$$

The elements $T_{nn'}$ of the T-matrix are found from

$$f_n = \sum_{n'} T_{nn'}a_{n'}. \tag{8}$$

It has been shown[1,5] that these elements are given by

$$T = -(\mathrm{Re}\,Q)\,Q^{-1} \tag{9}$$

where the elements of the auxiliary matrix Q are given by

$$Q_{nn'} = -k \iint_S d\vec{S}' \cdot \vec{\nabla}' \psi_n(\vec{r}') \, \mathrm{Re}\, \psi_{n'}(\vec{r}') \tag{10}$$

whenever the Neumann B.C. is satisfied on S i.e., $\hat{n} \cdot \nabla \psi = 0$, or given by

$$Q_{nn'} = k \iint_S d\vec{S}' \cdot \left[\vec{\nabla}' \, \mathrm{Re}\, \psi_{n'}(\vec{r}') \right] \psi_n(\vec{r}') \tag{11}$$

whenever the Dirichlet B.C. is satisfied on S, i.e., $\psi(\vec{r}) = 0$. If the object has spherical shape, the integral in Equations (10) and (11) can be performed exactly, in closed form, and the T-Matrix elements in Equation (9) can be analytically determined. For other shapes, the integrations over S must be carried out numerically and the T-Matrix elements are then numerically determined. Once the scattered field is determined, the cross section is:

$$\frac{\sigma_B}{\pi a^2} = \frac{4}{a^2} \left(\frac{d\sigma}{d\theta} \right)_{\theta=\pi} = \left| \frac{2}{a} f_\infty(ka, \theta) \right|^2_{\theta=\pi} = \lim_{r \to \infty} \left| \frac{2r}{a} \cdot \frac{\psi^s}{\psi^i} \right|^2_{\theta=\pi}, \tag{12}$$

in normalized form. All the above is for a single scatterer. If there are two scatterers of surfaces S_1 and S_2 in the medium, then the analysis becomes more complicated since it requires two shifts of origins. These origin shifts, so common in solid state physics, are an immediate clue that one is eventually going to deal with addition theorems for (vector) spherical harmonics,[8] and the machinery originally developed in atomic physics to handle the coupling of two angular momenta vectors[9-15] (i.e., Clebsch-Gordan coefficients and/or Wigner 3-j symbols). Equation (1) still holds, but the integration is now over $S_1 + S_2$, and its upper result is for $\vec{r}$ outside S_1 and S_2, while the lower one is for $\vec{r}$ inside S_1 or S_2. Let 0 be an origin outside both scatterers, and let 0_1, 0_2 be origins inside S_1 and S_2, respectively. The incident field can still be expanded by Equation (7), where $\vec{r}$ is now the radius vector from 0, provided that ψ^i contains no sources inside a sphere centered at 0 and containing both S_1 and S_2. Expansions of ψ^i and of $g(k|\vec{r}-\vec{r}'|)$ are also required about both 0_1 and 0_2. Let $\vec{a}_1, \vec{a}_2$ be position vectors of 0_1, 0_2, relative to 0. Let $\vec{r}_1, \vec{r}_1''$ (or $\vec{r}_2, \vec{r}_2''$) be position vectors of a point interior to S_1, or of a point of the boundary of S_1, (or of S_2), respectively, relative to 0_1 (or to 0_2). Let $\vec{r}_1', \vec{r}_2'$ be position vectors of a boundary point of S_1, S_2, relative to 0. The two expansions equivalent to Equation (4) are[5]:

$$g(k|\vec{r}-\vec{r}_1'|) = ik \sum_n \psi_n(\vec{r}_1'') \, \mathrm{Re}\, \psi_n(\vec{r}_1), \tag{13}$$

$$g(k|\vec{r}-\vec{r}_2'|) = ik \sum_n \psi_n \left[\vec{r}_2'' - (\vec{a}_1 - \vec{a}_2) \right] \mathrm{Re}\, \psi_n(\vec{r}_2). \tag{14}$$

where $\vec{r}=\vec{r}_1+\vec{a}_1$. It follows that the translation properties[8,13] of Re ψ_n and ψ_n are required to handle these origin shifts. Those of Re ψ_n are given by:

$$Re\,\Psi_n(\vec{r}_1+\vec{a}_1) = \sum_{m'}^{} R_{mm'}(\vec{a}_1)\, Re\,\Psi_n(\vec{r}_1). \tag{15}$$

The matrix $R_{m'}(\vec{a}_1)$ takes care of the translation and it is borrowed from elsewhere[8]; it is given here in terms of another matrix τ referring to a general translation $\vec{a}=(a,\eta,\psi)$, viz

$$R_{\sigma mn,\sigma' m'n'}(\vec{a}) \equiv \begin{cases} (-1)^m \frac{1}{2}\sqrt{\epsilon_m \epsilon_{m'}}\,\Big[(-1)^{m'} \tau_{mn,m'n'}(a,\eta)\cos(m-m')\psi \\ \quad + (-1)^{\sigma} \tau_{mn,-m'n'}(a,\eta)\cos(m+m')\psi\Big] \quad (\sigma=\sigma') \\ (-1)^m \frac{1}{2}\sqrt{\epsilon_m \epsilon_{m'}}\,\Big[(-1)^{m'+\sigma'} \tau_{mn,m'n'}(a,\eta)\sin(m-m')\psi \\ \quad + \tau_{mn,-m'n}(a,\eta)\sin(m+m')\psi\Big] \quad (\sigma\neq\sigma'), \end{cases} \tag{16}$$

where τ is given by:

$$\tau_{mn,m'n'}(a,\eta) = \sum_{k=|n-n'|}^{n+n'} (-1)^{m'+n+(n+n'+k)/2}(2k+1)\,j_k(ka)\,P_k^{m-m'}(\cos\eta)\,*$$

$$*\sqrt{\frac{(2n+1)(2n'+1)[k-(m-m')]!}{[k+(m-m')]!}} \cdot \begin{pmatrix} n & n' & k \\ 0 & 0 & 0 \end{pmatrix} \cdot \begin{pmatrix} n & n' & k \\ m & -m & -(m-m') \end{pmatrix}, \tag{17}$$

and $\begin{pmatrix} j_1 & j_2 & j_3 \\ m_1 & m_2 & m_3 \end{pmatrix}$ is the Wigner 3-j symbol defined[11] as follows:

$$\begin{pmatrix} j_1 & j_2 & j_3 \\ m_1 & m_2 & m_3 \end{pmatrix} = (-1)^{n-n-m_3}$$

$$\times\left(\frac{(j_1+j_2-j_3)!(j_1-j_2+j_3)!(-j_1+j_2+j_3)!(j_1+m_1)!(j_1-m_1)!(j_2+m_2)!(j_2-m_2)!(j_3+m_3)!(j_3-m_3)!}{(j_1+j_2+j_3+1)!}\right)^{1/2} \tag{18}$$

$$\sum_k \frac{(-1)^k}{k!(j_1+j_2-j_3-k)!(j_1-m_1-k)!(j_2+m_2-k)!(j_3-j_2+m_1+k)!(j_3-j_1-m_2+k)!}.$$

The particular Wigner 3-j symbol $\begin{pmatrix} n & n' & k \\ 0 & 0 & 0 \end{pmatrix}$, vanishes if J = n+n'+k is odd. If J = even then

$$\begin{pmatrix} n & n' & k \\ 0 & 0 & 0 \end{pmatrix} = (-1)^{J/2} \sqrt{\frac{(J-2n)!\,(J-2n')!\,(J-2k)!}{(J+1)!}} \cdot \frac{(J/2)!}{(\tfrac{1}{2}J-n)!\,(\tfrac{1}{2}J-n')!\,(\tfrac{1}{2}J-k)!} \cdot \tag{19}$$

The form of the matrix $R(\vec{a})$ given in (16) - (19) is quite general since it refers to a general translation $\vec{a}=(a,\eta,\psi)$. For the particular case[5,8] of a translation "d" along the z-axis, it reduces to

$$R(\pm d)_{\sigma m n,\,\sigma' m' n'} = \sum_{k=|n'-n|}^{|n'+n|} (-1)^{m+n+(n+n'+k)/2} (2k+1)(\pm 1)^k \cdot \tag{20}$$

$$\cdot j_k(kd)\sqrt{(2n+1)(2n'+1)} \begin{pmatrix} n & n' & k \\ 0 & 0 & 0 \end{pmatrix} \begin{pmatrix} n & n' & k \\ m & -m & 0 \end{pmatrix} \delta_{\sigma\sigma'}\,\delta_{mm'} \begin{cases} 1 & m>0 \\ 1 & m=0,\ \sigma=e \\ 0 & m=0,\ \sigma=o\,; \end{cases}$$

which still contains the 3-j Wigner symbols defined above. We still require the translation properties of ψ_n, which is of the form

$$\Psi_n[\vec{r}_2'' - (\vec{a}_1-\vec{a}_2)] = \sum_{n'} \sigma_{nn'}(-\vec{a}_1+\vec{a}_2)\, Re\,\Psi_{n'}(\vec{r}_2'') \,, \tag{21}$$

where the matrix $\sigma_{nn'}$ takes care of the translation of origins. It turns out that $\sigma_{nn'}$ is exactly the same as the matrix $R_{nn'}$ except that the Bessel function $j_k(ka)$ appearing in Equation (17) is now to be replaced by the Hankel function $h_n^{(1)}(ka)$. With that single change, Equations (16)-(20), remain as before also for $\sigma_{nn'}(-\vec{a}_1+\vec{a}_2)$.

If Equations (7), (13), (14), (15), and (21) are substituted into Equation (1), the result is an expression in which the coefficients of $Re\,\psi_n(\vec{r}_1)$ can be set equal, and this yields:

$$R^c(\vec{a}_1)\,\vec{a}=i\rho^1\alpha^1+i\sigma(-\vec{a}_1+\vec{a}_2)\,Re\,Q^2\alpha^2, \tag{22}$$

where $\vec{r}=\vec{r}_1+\vec{a}_1$ and the Q^i (i=1,2) are given by Equations (10) and (11) depending on the type of B.C. used, and the integration is over S_1. The same procedure for $\vec{r}=\vec{r}_2+\vec{a}_2$ in S_2 yields the analogous result,

---

NOTE: Let $\vec{J}_1$ and $\vec{J}_2$ be two angular momenta vectors of magnitude j_1 and j_2. The sum of these momenta is: $\vec{J}=\vec{J}_1+\vec{J}_2$, of magnitude j. If m_1, m_2 (with $m=m_1+m_2$) are the eigenvalues of two suitable eigenfunctions $X(j_1m_1)$, $X(j_2m_2)$ respectively associated with the $\vec{J}_1, \vec{J}_2$, then the eigenfunction of $\vec{J}$, in terms of those of $\vec{J}_1$ and $\vec{J}_2$ is:

$$X(jm) = \sum_{\alpha} C(j_1j_2j;\, m_1m_2m)\, X(j_1m_1)\, X(j_2m_2)\,.$$

The coefficients are the Clebsh-Gordan coefficients which are proportional to the Wigner 3-j symbols. If $\vec{J}_1$ and $\vec{J}_2$ were not coupled, each precessing independently about $\vec{J}$, then the eigenfunction of $\vec{J}$ in terms of those of $\vec{J}_1$ and $\vec{J}_2$ would be: $X(j_1m_1)\,X(j_2m_2)$.

$$R^{+}(\vec{a}_2)\vec{a}=i\,Q^2\alpha^2 + i\sigma(i\vec{a}_2 + \vec{a}_1)\;ReQ^1\alpha^1 \qquad (23)$$

where the α^i are the expansion coefficients over each S_i. If we now consider the scattered field expansion in Equation (6) together with Equation (13) and use $\vec{r}_i'=\vec{r}_i''+\vec{a}_i$ (i=1,2), we find,

$$f=iR(\vec{a}_1)Re\;Q^1\alpha^1-iR(\vec{a}_2)ReQ^2\alpha^2. \qquad (24)$$

Solving equations (22) and (23) for α^1 and α^2 in terms of $\vec{a}$ and substitution into equation (24) yields the total T-Matrix for the two scatterers, T_{12}, which is

$$T_{12}=\sum_{\substack{i,k=1\\ i\neq k}}^{2} R(\vec{a}_i)T_i\left[1-\sigma(-\vec{a}_i+\vec{a}_k)T_k\sigma(-\vec{a}_k+\vec{a}_i)T_i\right]^{-1} * \qquad (25)$$
$$* \left[1+\sigma(-\vec{a}_i+\vec{a}_k)T_k R(\vec{a}_i-\vec{a}_k)\right]R(-\vec{a}_i)\;,$$

in terms of the translation matrix R in equations (16) - (19), where σ is obtained from R by replacing j_n by $h_n^{(1)}$, and in terms of the T-Matrices of the individual scatterers. For two identical spherical scatterers separated a distance $2\vec{d}$ = 2d $\hat{e}_z$ along the z-axis, the two T-matrices are the same and the result simplifies to:

$$T_{12}=t_1(-\vec{d})+t_2(\vec{d}) \qquad , \qquad [\vec{a}_1=-\vec{d},\quad \vec{a}_2=+\vec{d}.] \qquad (26)$$

where

$$t_1(\vec{d})=R(\vec{d})\,T[1-\sigma(-2\vec{d})\,T\sigma(2\vec{d})\,T]^{-1}[1+\sigma(-2\vec{d})\,TR(2\vec{d})]\,R(-\vec{d})\,. \qquad (27)$$

The simplest expression for this result is:

$$T_{12}=R(\vec{d})\,[TD_+M_-]\,R(-\vec{d})+R(-\vec{d})\,[TD_-M_+]\,R(+\vec{d})\,, \qquad (28)$$

where

$$D_\pm=[1-\sigma(\mp2\vec{d})\,T\sigma(\pm2\vec{d})\,T]^{-1} \qquad (29)$$

$$M_\mp=[1+\sigma(\mp2\vec{d})\,TR(\mp2\vec{d})]\,, \qquad (30)$$

where R is as given in (20), and σ is just like it with the j_n replaced by $h_n^{(1)}$. The Wigner 3-j symbols are as defined in equations (18) and (19). It should be remarked that both R and σ are orthogonal, viz.,

$$R^{+}(\vec{a})=R(-\vec{a}) \quad and \quad \sigma^{+}(\vec{a})=\sigma(-\vec{a})\,, \qquad (31)$$

and that the following addition theorem holds:

$$\sigma(\vec{a}+\vec{R}) \;=\; \sigma(\vec{R})\,R(\vec{a}) \;=\; R(\vec{a})\,\sigma(\vec{R}) \qquad (a<R)\,. \qquad (32)$$

For an elastic object in a fluid,[16], the (single-scatterer) T-matrix is not the one given by equation (9) and either (10) or (11), but rather by

$$T = -Re[QR^{-1}P]\,[QR^{-1}P]^{-1} \quad , \tag{33}$$

where the matrix $\tilde{Q} \equiv QR^{-1}P$ now plays the role of the old matrix Q in the acoustic case. The matrices P, R, Q required here to construct $\tilde{Q}$, and ultimately T are given elsewhere.[6,16] For the case of an elastic shell in a fluid, the pertinent T matrix is

$$T = -\left(Q_{RR} + Q_{RO}T_2\right)M^{-1}P\left[\left(Q_{OR} + Q_{OO}T_2\right)M^{-1}P\right]^{-1} \tag{34}$$

where $M \equiv R_R + R_O T_2 + i\,T_2$, and the various auxiliary matrices contained in this expression needed to construct T have been given elsewhere[17,18]. Various other T-matrices have been constructed for elastic inclusions in elastic media,[19] multilayered scatterers,[20,21] and others.[22] They can all be used in conjunction with the two-scatterer formulation given above.

II. AN ELASTIC STRUCTURE NEAR THE SEA SURFACE

We consider an elastic sphere (WC) and an elastic spherical shell near the sea surface being insonified from below by a plane c.w. acoustic wave. We use the method of images and assume the sphere is a distance d below the sea surface, and its virtual image is a distance d above it. We can use the methodology described above for two scatterers. This methodology will make use of the T-Matrix in equation (33) for the elastic sphere, and in equation (34) for the elastic shell. The spherical geometry is used for simplicity since the T-Matrix method could handle almost any arbitrary shell/solid shape. The method of images takes care of the type of boundary one has in between the sphere and its image. If the boundary is rigid - a good first approximation for a flat ocean bottom - the Green's functions of the object and its image are added, which is reflected in the sum of the two terms for the T_{12} - matrix in equation (26). If the boundary is soft (i.e., Dirichlet B.C.), then we should take the difference of the two terms in equation (26). We will show calculations below for both these cases, although the most important one, and the one depicted in Figure 1, is the one in which the intermediate boundary is a pressure release surface, such as that of the sea.

All our frequency-domain calculations will produce moduli of form functions $|f_\infty|$ (c.f., equation (12)). These will yield backscattering cross sections after squaring. All our time domain ($\tau \equiv ct/a$) calculations are obtained by means of[23,24]:

$$rp_{sc}(\tau) = \frac{1}{2\pi}\int_{-\infty}^{+\infty} f_\infty(x,\pi)\,G(x)\,e^{ix\tau}dx, \tag{35}$$

where G(x) is the spectrum (i.e., the Fourier transform) of whatever incident pulse is used.[25] In the case of very broad incident spectra, say, G(x) = 1, the time response approximates the inverse Fourier transform of $f_\infty(x)$, which is the "impulse response" of the scatterer, which we plot below.

III. NUMERICAL RESULTS

Numerous calculations of form-functions of spherical shells in unbounded media have been found by us in earlier work.[26] We are here concerned with a WC solid sphere and a thin spherical aluminum shell, near the boundary shown in Figure 1. If the separating boundary is rigid we add the two terms in equation (26) as discussed above. If it is pressure-release, we will subtract those two terms. Figure 2 shows the form-function of an elastic (WC) sphere in water in the band: $2 \le ka \le 10$, at various distances from a bounding rigid interface measured by the quantity R which is proportional to the distance to the boundary. There are two observable resonance features near 7 and 9 superimposed on smooth rigid (RST) background, as one would expect of a WC-sphere. These features are associated with the Rayleigh (R) and the first of the Whispering Gallery (WG) modes. As the sphere approaches the boundary (i.e., R=4, center; and R=2, bottom) the resonance peaks remain essentially at the same places, but they become broader and harder to distinguish from the level of a rising background. Thus, proximity to a rigid boundary tends to wash-out the resonances. Figure 3 is the same as Figure 2 but now the boundary is a soft, or pressure release, surface. As the WC sphere approaches the soft boundary (R=4, center; R=2, bottom) the pattern becomes considerably more distorted than in Figure 2 for the rigid boundary. The dips seen in the top plot at 7 and 9 now become peaks barely rising above the newly distorted backgrounds. The background gains in internal structure with proximity to the soft interface, but the resonances are also washed out, even more than when the interface was rigid. Figure 4 shows the late-time response (i.e., $50 \le \tau = ct/a \le 200$) as the WC sphere approaches a pressure-release boundary. These time domain calculations are performed by means of equation (35) and the corresponding form-function. As the sphere gets closer to the soft boundary (viz., center, R=4; bottom, R=2), the wave-packet structure of the response fades away, although a strong feature at $\tau = 170$ seems to remain always present. The amplitude of the displayed oscillations are about 10 times weaker than if the boundary had been rigid -- although we do not show that case here. Again, proximity to the boundary, particularly a soft one, washes out the significant features in the time-response, even when the boundary is an ideal, perfectly flat one. Figures 5 and 6 deal with a thin spherical aluminum shell (h/a=0.1%) in water, near a soft, or pressure release, boundary. Figure 5 (top) gives the form-function for the shell in a boundless medium[18], as one would have found it away from boundaries. This pattern is recovered in the presence of a pressure-release boundary if the distance of the shell from the boundary exceeds R=8 (i.e., 8 diameters away). As the shell approaches the soft boundary (i.e., R=4, center; R=2, bottom) its form-function becomes appreciably distorted. The resonance features at 4.2 and 8.3 persist, but the first one splits into two, while the backgrounds seem to decrease at high-frequencies. Figure 6 shows the late-time response (viz., $50 \le \tau = ct/a \le 200$) of the same aluminum spherical

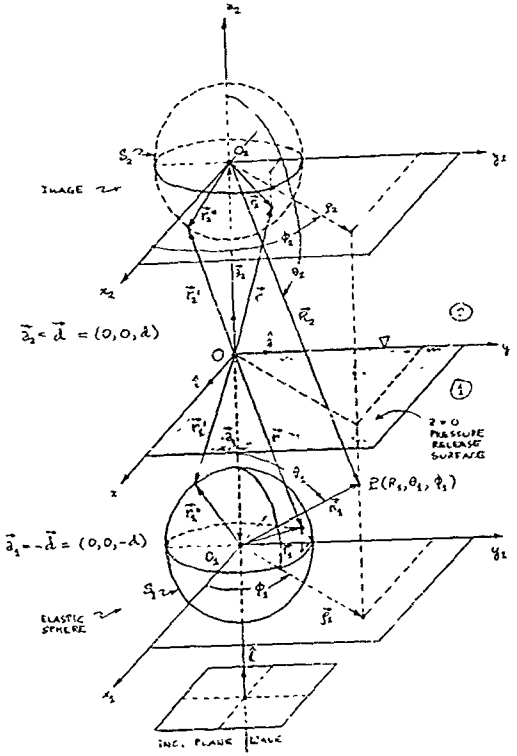

FIG. 1. The geometry of the object, its image and the separating boundary. All pertinent vectors are shown.

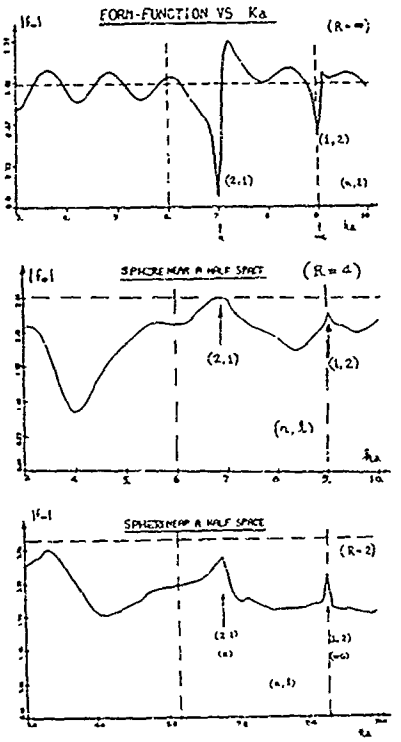

FIG. 2. Form function of a solid (WC) sphere approaching a rigid boundary. The sphere is very far away (R=∞) on top, and becomes closer (R=4, center; R=2, bottom), in the lower plots.

shell. The late-time response is dominated by the resonances of the shell, particularly the ones within the band: $3 \le ka \le 10$, as shown in Figure 5. As the shell approaches the pressure-release interface (i.e., R=4, center; R=2, bottom) there are substantial changes in the time-response. The amplitude of some of the later wave-packets increases with proximity to the boundary, although, in general, the entire response is weak, and much weaker than in the case of rigid interface.

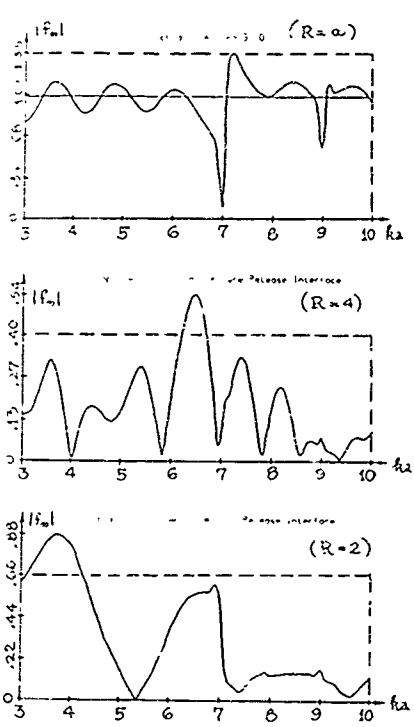

FIG. 3. Form-function of a solid (WC) sphere approaching a pressure release boundary. Again R=∞ (top); R=4 (center) and R=2 (closest, bottom).

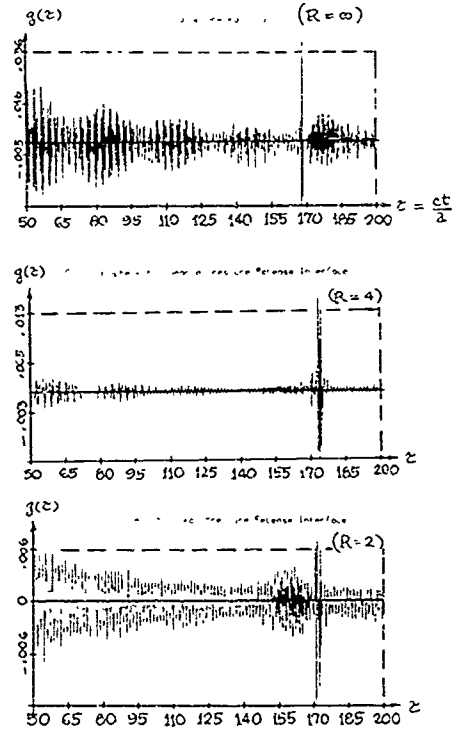

FIG. 4. Late-time response from the WC sphere in Fig. 3 as it approaches a soft boundary under the same conditions (τ=ct/a).

IV. CONCLUSIONS

The resonance features present in the form-functions or backscattering cross-sections (BSCS) of submerged elastic objects change as these objects get close to environmental boundaries. In general, the cross-sections and the temporal responses of elastic solid bodies and elastic shells become distorted near boundaries, and take on values quite different from their values in free-space or deep waters. The present study quantitatively describes those differences and graphically displays specific distortions for a given metal sphere and a specific thin spherical shell at various distances from an idealized model of the sea surface (or bottom). The approach used was the method of images

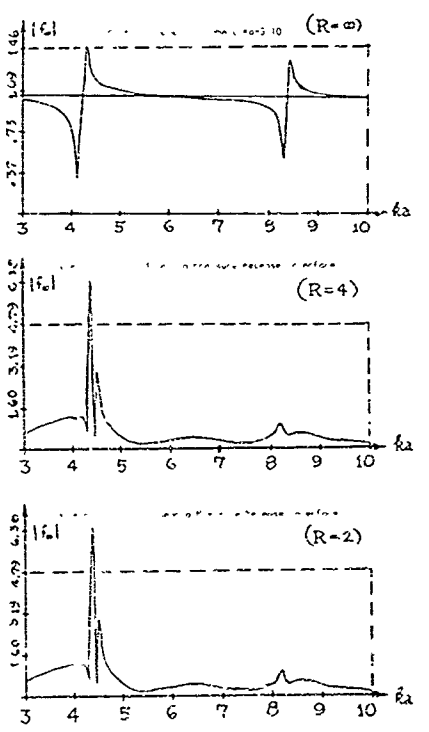

FIG. 5. Form-function of an aluminum spherical shell (h/a · ·1%) approaching a soft boundary. This is the shell counterpart of Fig. 3.

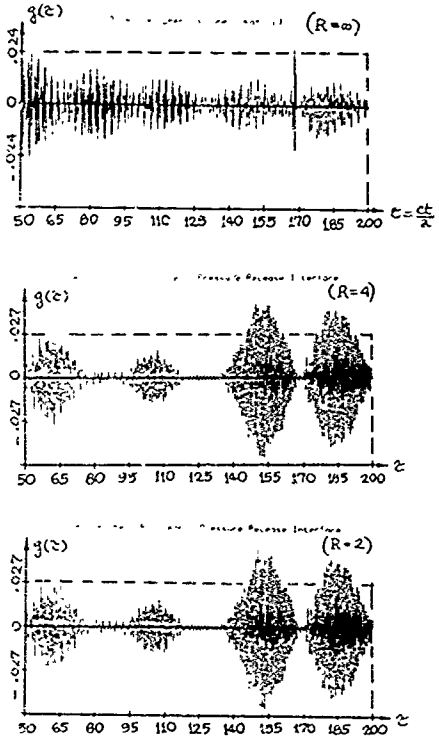

FIG. 6. Late-time response from the spherical aluminum shell as it gets closer to a pressure release interface. This is the shell counterpart of Fig. 4.

combined with a two-body scattering formulation that determined the T-matrix of two objects insonified by acoustic waves when the T-matrix of each individual object was either known or calculable. In our numerical results we noticed the splitting of certain resonances ("bifurcations"?) into two components as the structure approached the boundary. In general, proximity to the sea surface tends to wash-out or smooth-out the oscillatory nature of the BSCS. That oscillatory nature is due to resonances of the object and is essential for target-recognition purposes. In the time-domain, the boundary influence seems to be confined to a "skin-layer," bounded by R≤4. The free-space form-functions (i.e., Figures 2,3, and 5 (tops)) in the absence of boundaries

are recovered from the present general formulation when the objects are about 4-6 diameters away from the interface. Finally, and obviously, these distorting efforts in the BSCSs will make any target-recognition scheme substantially less effective for scatterers that remain indefinitely near environmental boundaries. Fortunately, the previous target-ID capabilities will be recovered at a few characteristic distances (i.e., diameters) away from those interfaces.

V. ACKNOWLEDGEMENTS

Thanks are due to the Naval Surface Warfare Center (NAVSWC) Independent Research Program Office, to the Naval Research Laboratory (NRL) Core Research Program, and to the Office of Naval Research for support of this work.

REFERENCES

1. P.C. Waterman, "New Formulation of Acoustic Scattering," J. Acoust. Soc. Amer., 45, 1417-1429, (1969).

2. B. Baker and E. Copson, The Mathematical Theory of Huyghen's Principle, Oxford, Clarendon Press, England, (1953).

3. P. Morse and H. Feshbach, Methods of Theoretical Physics, McGraw Hill, New York (1953), (See Chapter 13).

4. J. Jackson, Classical Electrodynamics, Wiley, New York, (1962).

5. B. Peterson and S. Ström, "Matrix Formulation of Acoustic Scattering from an Arbitrary Number of Scatterers," J. Acoust. Soc. Amer., 56, 771-780, (1974).

6. M. Werby and R. Evans, "Scattering from Objects Submerged in Unbounded and Bounded Oceans," IEEE J. Ocean. Engr., OE- 12, 380-394, (1987).

7. M. Werby and G. Gaunaurd, "Resonances in the Backscattered Echoes from Elastic Shells Near an Interface," in Elastic Wave Propagation, 393-399, North Holland/Elsevier Publishers, (1989).

8. M. Danos and L. Maximon, "Multipole Matrix Elements of the Translation Operator," J. Mathem. Phys., 6, 766-778, (1965).

9. A. Edmonds, Angular Momentum in Quantum Mechanics, Princeton Univ. Press, Princeton, New Jersey, (1957).

10. M. Rose, Elementary Theory of Angular Momentum, J. Wiley and Sons, Inc., New York, (1961).

11. M. Rotenberg et al., The 3-j and 6-j Symbols, Technology Press, Cambridge, Massachusetts, (1959).

12. E. Wigner, Group Theory and its Application to the Quantum Mechanics of Atomic Spectra, Academic Press, New York, (1959).

13. R.A. Sack, "Three-dimensional Addition Theorem for Arbitrary Functions Involving Expansions in Spherical Harmonics," J. Mathem. Phys., 5, 252- 259, (1964).

14. R. New and T. Eisler, Acoustic Radiation from Multiple Spheres," J. Sound and Vibrat., 22, 1-17, (1972).

15. E. Condon and G. Shortly, Theory of Atomic Spectra, Cambridge Univ. Press, London (1951).

16. A. Boström, "Scattering of Stationary Acoustic Waves by an Elastic Obstacle Immersed in a Fluid," J. Acoust. Soc. Amer. 67, 390-398, (1980).

17. G. Gaunaurd and M. Werby, "Resonance Response of Submerged, Acoustically excited, Thick and Thin Shells," J. Acoust. Soc. Amer., 77, 2081-2093, (1985).

18. G. Gaunaurd and M. Werby, "Proper Background Choice in Resonance Scattering by Submerged Elastic Shells," Intern. J. Solids and Structures 22, 1149-1159, (1986).

19. A. Boström, "Scattering by a Smooth Elastic Obstacle," J. Acoust. Soc. Amer., 67, 1904-1913, (1980).

20. A. Boström, "Multiple Scattering of Elastic Waves by Bounded Obstacles," J. Acoust. Soc. Amer., 67, 399-413, (1980).

21. B. Peterson and S. Ström, "Matrix Formulation of Acoustic Scattering from Multilayered Scatterers," J. Acoust. Soc. Amer., 57, 2-13, (1975).

22. G. Kristensson and S. Ström, "Scattering from Buried Inhomogeneities - A General 3-Dimensional Formalism," J. Acoust. Soc. Amer., 64, 917-936, (1978).

23. E. Kennaugh and D. Moffatt, "Transient and Impulse Response Approximations," Proc., IEEE Vol. 53, 893-901, (1965).

24. R. Hickling and R. Means, "Scattering of FM-Pulses by Spherical Elastic Shells in Water," J. Acoust. Soc. Amer., 44, 1246-1252, (1968).

25. G. Gaunaurd and W. Wertman, "Transient Acoustic Scattering by Fluid-Loaded Elastic Shells," Intern. J. Solids and Structures 27, 699-711, (1991).

26. G. Gaunaurd and M. Werby, "Sound Scattering by Resonantly Excited, Fluid-Loaded, Elastic Spherical Shells," J. Acoust. Soc. Amer., 90, 2536-2550, (1991) (and references therein).